

Supplemental Information

**Spatiotemporal Control of Lipid Conversion, Actin-
Based Mechanical Forces, and Curvature Sensors
during Clathrin/AP-1-Coated Vesicle Biogenesis**

Mihaela Anitei, Christoph Stange, Cornelia Czupalla, Christian Niehage, Kai Schuhmann, Pia Sala, Aleksander Czogalla, Theresia Pursche, Ünal Coskun, Andrej Shevchenko, and Bernard Hoflack

SUPPLEMENTAL DATA

SUPPLEMENTAL EXPERIMENTAL PROCEDURES

Reagents: GTP γ S (Guanosine 5'-O-(3-Thiotriphosphate)), ATP, creatine phosphokinase, creatine phosphate and complete protease inhibitors were from Roche Diagnostics, Germany. Inhibitors: latrunculin B (Calbiochem/Merck, Germany), fumonis B1 (Cayman Chemical, MI, USA), phorbol 12,13-dibutyrate (PDBu) (Sigma-Aldrich, Germany), and rapamycin (LC laboratories, MA, USA). Fluorescent Alexa-fluorophore labeled secondary antibodies, DAPI and DiI-C16 were from Molecular Probes/Life Technologies (Germany). HRP-conjugated secondary antibodies were from Dianova, Germany. Primary antibodies: mouse anti-arfaptin-2 (clone 2B5) (Sigma-Aldrich); goat anti-arfaptin-1 (I-19) and rabbit anti-PLCB3 (C20) (Santa Cruz Biotechnology, TX, USA); rabbit anti-PIP5K1A (15713-1-AP, Proteintech Group, IL, USA); mouse anti-AP-1- γ (clone 88), anti-GM130, anti-RAC1 and anti-tubulin b (BD Biosciences, CA, USA), rabbit anti-p34-Arc/ARPC2 (Millipore), mouse anti-GAPDH (Acris Antibodies, Germany), rabbit anti-clathrin heavy chain (ab21679, Abcam, UK), rabbit anti-PPAP2A and rabbit anti-PLD1 (EP1506Y) (GeneTex, CA, USA), mouse IgM anti-GTP-RAC1 (New East Biosciences, PA, USA), sheep anti-TGN46 (Novus Biologicals, CO, USA), mouse IgM anti-PI[4,5]P2 (Echelon Biosciences, UT, USA), anti-GFP clone 7.1 and 13.1 (Roche Life Science, Germany), mouse anti-human transferrin receptor (clone H68.4) (Zymed, Life Technologies).

DNA constructs: The mammalian expression vectors pEGFP-N3, pEGFP-C1, and pmCherry-C1 were from Takara Bio Europe/Clontech (France). Plasmids used: YFP-DBD (Addgene plasmid 14874)(Gallegos et al., 2006); GFP-PLC δ -PH (Addgene plasmid 21179)(Stauffer et al., 1998), GFP-CERT(Kawano et al., 2006), GFP-PH-FAPP1(Balla et al., 2005), mRFP-FKBP12-hSac1, mRFP-FKBP12 and CFP-Tgn38-FRP(Szentpetery et al., 2010), pEGFP-ciMPR, mCherry-ciMPR and pmRFP-ciMPR(Waguri et al., 2003), GFP-actin (BD Bioscience, CA, USA), myc-PIP5K1A(Rozelle et al., 2000), HA-Rac1V12 (Tobias Heckel, Roche Diagnostics, Switzerland), pCyPet RAC1Q71L- (Addgene plasmid 22783)(Machacek et al., 2009).

The coding sequence of human arfaptin-1 was amplified from HeLa cell cDNA and its large splice variant (373 aa) was cloned into pEGFP-C1 and into pmCherry-C1. The coding sequence of human arfaptin-2 was amplified from HeLa cell cDNA and was cloned into pGFP-N3.

Cell lines and transfection: HeLa and HEK-293T cell lines were from the American Type Culture Collection (LGC Standards GmbH, Germany). GFP-MPR expressing HeLa cells were described in(Waguri et al., 2003). BSC-1 cells stably expressing GFP-AP-1- σ were a gift from Tomas Kirchhausen (Harvard Medical School, MA, USA). HEK cells stably expressing GFP-arfaptin-2, GFP-actin, YFP-DBD or GFP-PLC δ -PH were generated as described below. Cells grown in one well of a 24-well plate were transfected with 1 μ g plasmid DNA. Two days after transfection, cells were detached with trypsin and seeded into 10 cm dishes containing medium supplemented with 0.8 mg/ml Geneticin (Gibco, Life Technologies). After 2-3 weeks, single clone-derived colonies were picked and transferred into wells of a 24-well plate. Clones were individually analyzed for expression by fluorescence microscopy and/or Western blot, and suitable clones were grown with 0.3 mg/ml Geneticin. All cell culture reagents were purchased from Gibco/Life Technologies.

RNA interference: All small interfering RNAs (siRNAs) were supplied as annealed Silencer Select Pre-Designed siRNAs (Ambion//Life Technologies) or stealth siRNA (Invitrogen/Life Technologies) and were stored at -20° C, as 20 μ M stock solutions in water.

siRNA sequences:

siArfaptin-1a (Entrez GeneID: 27236; 5'-GAAAUCCAGUGACUAGUAtt-3');
siArfaptin-1b (Entrez GeneID: 27236; 5'-GGGUGUUAUUGAAGCAGGAtt-3');
siArfaptin-2a (Entrez GeneID: 23647; 5'-GGACCCAACCUCAAUGAAAtt-3');
siArfaptin-2b (Entrez GeneID: 23647; 5'-CAACUGUUAUCAGAACGAUtt-3');
siPIP5K1A_1 (Entrez GeneID: 8394; 5'-CAAGAUCGGUAAAAAUGCtt-3');
stealth siPIP5K1A_2 (5'-GCGUUCACCUUGGUCGUCCUGAUGU);
siPLCB3_1 (Entrez GeneID: 5331; 5'-GCAUAACACCUAUCUCACUtt-3');
stealth siPLCB3_2 (5'-GGCUUCACUUCGCAU UGCAGCCUUU-3');
stealth siPLD1 (Entrez GeneID: 5337, 5'-CCAACUUUCUCAAAGAUCGAUU-3');
stealth siPLD2 (5'-CAGGUGGUGGGC ACCGAAAGAUUA-3');
stealth siPPAP2A (Entrez GeneID: 8611, 5'-UAGUAUUCAAUGUAACCAUCGCUGC-3').

siNon2 represents Silencer Select Negative Control #2 (Ambion/Life Technologies). The siRNAs were delivered into cells at a final concentration of 10 nM (24 or 6 well plates) or 20 nM (10 cm plates), using INTERFERIN reagent (Polyplus Transfection, France) according to supplier's protocol. Cells were treated with siRNAs for 72 h prior to analysis.

Cytosol preparation. Mouse brains (female CD1, Biomedical Service Unit of the MPI-CBG, Dresden, Germany) were dissected, the cerebellum and the meninges were removed, and the remaining brain tissue was homogenized, using a dounce tissue grinder (Wheaton Science Products, NJ, USA), in 3 volumes of homogenization buffer (25 mM HEPES, pH 7.2, 125 mM potassium acetate, 2.5 mM magnesium acetate, supplemented with 2 mM Na₂V₂O₄, 5 mM NaF, 50 mM beta-glycerol phosphate and complete protease inhibitor mix). The homogenate was centrifuged at 200,000 g for 2 h (SW60 rotor, Optima LE-80K Ultracentrifuge, Beckman Coulter, CA, USA) to pellet insoluble components. To obtain cytosolic extracts from HeLa or HEK cell lines, cells grown to confluence in 10 cm plates were washed with cold PBS and detached using a cell lifter. Cells were pelleted by 5 min centrifugation at 450 g, and suspended in 100 µl volumes of homogenization buffer. Cells were homogenized with a syringe by repeatedly passing them through a 27 Gauge needle. The homogenate was centrifuged at 10,000 g for 15 min, the supernatant was recovered and centrifuged at 200,000 g for 1 h (TLA55 rotor, Optima Max Ultracentrifuge, Beckman Coulter, CA, USA) to pellet insoluble components.

Liposome preparation: All lipids were from Avanti Polar Lipids Inc. (AL, USA) and the concentrations were confirmed by total phosphorus assay (Rouser et al., 1966). Phosphatidylcholine (PC, 1,2 DOPC) or sphingomyelin (SM, porcine brain extract), phosphatidylethanolamine (PE, porcine brain extract), phosphatidylserine (PS, porcine brain extract), cholesterol (free cholesterol), maleimide lipid anchor (18:1 PE-MCC) and PI[4]P (porcine brain extract) or (when indicated) PI[4,5]P₂ (porcine brain extract) were mixed in a molar ratio of 41.5% : 31.5% : 10.5% : 10.5% : 1% : 5%. The incorporation of charged lipids into liposomes as well as reproducibility was confirmed by zeta potential measurements (Malvern, ZetaSizer Nano ZS). Where not specifically indicated, liposomes contained PC. For GUV formation, DiI-C16 was added in a molar ratio of 0.02%. Lipids were dried with a stream of Nitrogen. The lipid film was rehydrated with coupling buffer (20 mM Hepes pH 7.2, 125 mM potassium acetate, 1 mM EDTA) to a lipid concentration of 2 µmol/ml. Liposomes were formed by extrusion through an 800 nm membrane (PC MB 19 mm, 0.8 µm, Whatman, GE Lifesciences, Germany) using a Mini-Extruder from Avanti Polar Lipids Inc. (AL, USA). Coupling of the gE/gpI cd peptide to freshly prepared 18:1 PE-MCC containing liposomes took place at room temperature for 1 h in presence of 1 mM TCEP (tris(2-carboxyethyl)phosphine). The gE/gpI cd peptide (NH₂-CGKRMRVKAYRVKSPYNQSMYYAGLPVDDFEDSESTDTEE-COOH) was synthesized by EZBiolab (IN, USA). Alternatively, the gE/gpI cd was cloned in a modified pET28 expression plasmid (Niehage et al., 2014) and the 6xHis-MBP--tagged peptide was purified by affinity chromatography. Subsequently, the affinity tag was removed by TEV protease cleavage and the peptide was further purified by size exclusion chromatography.

Protein recruitment onto liposomes: Cytosolic extract (protein concentration 4 mg/ml) was supplemented with 100 µM GTPγS, and (when indicated) ATP-regeneration system (1 mM ATP, 10 mM creatine phosphate, 10 µg/ml creatine kinase) and 20 µM latrunculin B. Liposomes were added to a final concentration of about 200 nmol/ml. The mixture was incubated at 37°C for indicated times. Reaction was stopped by addition of 1 ml of cold recruitment buffer. Liposomes were separated from the cytosol mixture by centrifugation (20,000 g for 15 min). Pellets were resuspended in 25 µl of 2X Laemmli buffer, and analyzed by SDS-PAGE and Western blot.

For mass spectrometry analysis, we used 1 ml of mouse brain cytosol (protein concentration 10 mg/ml) and 100 µl liposomes (~100 µmol total lipid). After 25 min at 37°C, the reaction mixture was mixed with 4.5 ml of 65% (w/v) sucrose in recruitment buffer, and then transferred to a 14 ml ultracentrifugation tube. The mixture was overlaid with 5.5 ml of 40% (w/v) sucrose in recruitment buffer, then with 2 ml recruitment buffer, and then centrifuged (12 h, 35,000 RPM, 4°C) in a free-swinging rotor (SW-40), using an Optima LE80 ultracentrifuge. The sucrose interphase containing liposomes was recovered, and liposomes were harvested by centrifugation (20,000g, 15 min, 4°C). Pellets were re-suspended in 25 µl of 2X Laemmli buffer and analyzed by SDS-PAGE.

Mass spectrometry-based proteomic analysis: Control and treated samples were separated by SDS-PAGE side-by-side. Gel lanes were cut into 30 slices in parallel fashion. Protein digestion and in-gel ¹⁶O/¹⁸O-labeling was performed as described (Lange et al., 2010). In brief, gel pieces were incubated

with 100 ng trypsin (Promega, WI, USA) in the presence of H₂O¹⁸ (97% ¹⁸O, Campro Scientific GmbH, Germany) or H₂O¹⁶ as indicated, and paired samples were combined immediately before nano-LC-MS/MS analysis. Label-free sample preparation for mass spectrometry was done as described (Czupalla et al., 2006). Peptides were separated on an EASY-nLC nano-HPLC system (Proxeon, Denmark) equipped with a fused silica microcapillary C18 analytical column (3 µm, 100 Å, 10 cm x 75 µm i.d.) directly coupled to the nanoelectrospray source of a LTQ Orbitrap XL mass spectrometer (Thermo Fisher Scientific). Peptides were eluted with a 90 min gradient of 5-50% acetonitrile in 0.1% formic acid at 300 nL/min. Mass spectra were acquired in a data-dependent mode with one MS survey scan (resolution of 60,000) in the Orbitrap and MS/MS scans of the five most intense precursor ions in the LTQ. MS/MS spectra of ¹⁶O/¹⁸O-labeling experiments were processed and searched against the UniProtKB/SwissProt database (release 56.9, 412,525 sequences, 16,091 *Mus musculus* sequences) using a Mascot server (version 2.2, Matrix Sciences Ltd., UK). Search criteria were: taxonomy, mouse; mass tolerance of precursor and sequence ions, 10 ppm and 0.35 Da, respectively; modifications, cysteine carbamidomethylation, methionine oxidation, serine/ threonine/ tyrosine phosphorylation, and C-terminal ¹⁸O1- and ¹⁸O2-isotope labeling; maximum two missed cleavages. A protein was accepted as identified if the total Mascot score was greater than the significance threshold ($p < 0.05$) and if at least two unique peptides were detected. Based on decoy database searches, the false discovery rate was estimated to be $< 1\%$. Quantification was carried out using the Mascot Distiller Quantification Toolbox (version 2.2.1.2, Matrix Sciences) and was based on calculations of at least two unique tryptic peptides. Relative protein ratios were calculated from the intensity-weighted average of all peptide ratios. For most proteins, peptides were detected in separate, adjacent, gel slices. Based on the calculated protein scores, we excluded the gel slices with low scores ($< 25\%$ of the highest protein score calculated in one gel slice) and low peptide number ($< 25\%$ of the maximum number). The remaining values (high/low ratios) were averaged to obtain the global peptide ratio (Table S1).

The LC-MS workflow of label-free liposome recruitment experiments has been described in (Niehage et al., 2014). Briefly, samples were fractionated after SDS-PAGE by cutting full lanes into 12 slices, cysteins reduced, carbamidomethylated and proteins in-gel digested by trypsin in a 1:50 ratio. Peptides were separated on a 15 cm reversed-phase column (C18, 15 cm x 75 µm, 2 µm beads of 100-Å pore size; Dionex) within a 60 min gradient from 0.1% formic acid / 5% acetonitrile to 0.1% formic acid / 40% acetonitrile operated by an Ultimate 3000 HPLC system (Dionex). Mass spectrometry was performed with a LTQ Orbitrap XL mass spectrometer (Thermo Scientific), equipped with a nanoESI source (Proxeon). The top eight peaks in the mass spectra (Orbitrap; resolution, 60,000) were selected for fragmentation (CID; normalized collision energy, 35%; activation time, 30 ms, q-value, 0.25) with dynamic exclusion enabled (repeat count, 2; repeat duration, 10 s; exclusion duration, 20 s). MS/MS spectra were acquired in the LTQ in centroid mode. Proteins were identified using the MaxQuant software package version 1.2.2.5 (MPI for Biochemistry, Germany) (Cox and Mann, 2008) and UniProt database version 01/2012. Carbamidomethylation of cysteine was chosen as a fixed modification; acetylation of the N-terminus, deamidation of asparagine and oxidation of methionine as variable modifications. The MaxQuant result file was further processed in Perseus version 1.2.0.13 (MPI for Biochemistry, Germany). Proteins with at least one unique and two razor peptides were kept when present in at least two of three replicates. A t-test was performed with a threshold value of 0.001 and a slope value of the threshold curve of 0.2.

Data analysis of label-free experiments was done using MaxQuant version 1.2.2.5 (Cox and Mann, 2008). Peak lists were searched against a database containing 20,253 entries from the UniProtKB/Swiss-Prot human database (release 2011_02) and 255 frequently observed contaminants as well as reversed sequences of all entries and the search criteria listed above with the following exceptions: mass accuracy, 6 ppm and 0.5 Da for precursor ion and fragment ion mass tolerance, respectively; fixed and variable modifications, cysteine carbamidomethylation and methionine oxidation, respectively. Peptide identifications were accepted based on their posterior error probability until less than 1% reverse hits were retained while protein false discovery rates were $< 1\%$. Proteins were considered if at least two peptides were identified. All Mass Spectrometry data will be made available upon request.

Statistical Analyses were performed using Microsoft Excel for Mac and StatPlus Mac (AnalystSoft Inc., CA, USA). Data are shown as mean \pm SD or median \pm SD, and p-values were calculated using one-way Anova (* $p \leq 0.05$, ** $p \leq 0.005$).

Gene set enrichment analysis (GSEA) uses statistical methods (hypergeometric distribution) to establish if components of a particular subcellular/molecular pathway are over-represented among a defined set of genes. We performed GSEA using the software provided by the Broad Institute, CA, USA (<http://software.broadinstitute.org/gsea/index.jsp>) (Subramanian et al., 2005, Mootha et al., 2003).

Thin Layer Chromatography (TLC) of lipids. After the incubation of liposomes with mouse brain cytosol (protein concentration 4 mg/ml) for indicated times, lipids were immediately extracted using chloroform/methanol (10:1 v/v) (Folch et al., 1957), incubated for 20 min on ice, and centrifuged (5000 g, 4°C, 4 min). The upper, aqueous phase was re-extracted with chloroform/methanol/acetone/1 M HCl (2:1:0.5:0.1 v/v) (Dawson and Eichberg, 1965). All samples were kept on ice during the entire extraction procedure. The respective organic phases were pooled and subsequently evaporated under a nitrogen stream. Samples were then dissolved in 20 µl chloroform/methanol/acetone/1 M HCl (2:1:0.5:0.1 v/v) and loaded on silica gel 60 HPTLC plates (Merck KGaA, Germany) pre-coated with potassium oxalate (Gonzalez-Sastre and Folch-Pi, 1968). As mobile phase, we used either hexane/diethyl ether/acetic acid (80:20:1 v/v) for non-polar lipids, or chloroform/methanol/acetone/acetic acid/water (46:15:17:14:8 v/v) for polar lipids. Lipids were stained with 0.5 % primulin (in acetone/water 8/2 v/v) (White et al., 1998) and visualized in a laser scanner (Typhoon 9410, Amersham Biosciences) with a 457 nm excitation wavelength.

Mass spectrometry-based lipidomics. Synthetic lipid standards were purchased from Avanti Polar Lipids and Sigma-Aldrich. Other chemicals were of ACS, CHROMASOLV® Plus or LC-MS grade and purchased from Sigma-Aldrich. Lipids were extracted with methyl-tert-butyl ether (MTBE) as described (Matyash et al., 2008). After incubation with mouse brain cytosol (4 mg/ml) for indicated time points, liposomes in solution (200 µl total volume) were immediately added into a 2 ml safe-lock Eppendorf tube together with 1 ml MTBE /methanol (10:3; v:v) mixture, containing internal standards: 680 pmol SM 18:1:1/12:0; 1310 pmol PC 12:0-13:0; 421 pmol PE 12:0-13:0; 318 pmol PS 12:0-13:0; 847 pmol FC-D7; 55 pmol PI[4]P4 16:0-16:0 and 173 pmol DAG-D5 17:0-17:0. The mixtures were shaken for 90 min (4°C) and centrifuged for 5 min at 13,400 rpm at 4°C. The upper organic phase was transferred to a glass vial and dried under vacuum. Prior to their analysis by mass spectrometry, lipid extracts were dissolved in isopropanol/methanol/chloroform mixture (4:2:1, v:v:v) with 7.5 mM ammonium formate to a final concentration of 20 µM. Shotgun lipidomics analyses were performed on a Q Exactive mass spectrometer (Thermo Fisher Scientific, Germany) equipped with a robotic nanoflow ion source TriVersa NanoMate (Advion BioSciences, Ithaca, NY). Samples were analyzed in technical replicates by broad band FT MS+ (t = 30s, range of m/z 350-1100, mass resolution $R_{m/z200} = 140.000$, AGC = $3 \cdot 10^6$), targeted SIM FT MS+ (t = 150s, m/z 400-1000, isolation width = 20 Th, step size = 10 Th, $R_{m/z200} = 140.000$, AGC = $5 \cdot 10^4$) followed by targeted HCD FT MS/MS (isolation width = 1 Th, $R_{m/z200} = 140.000$, AGC = $2 \cdot 10^4$). Normalized collision energy for targeted MS/MS of PI[4]P, cholesterol and DAG was set to 12% and 20%, respectively. Lipid species were quantified from pre-processed stitched SIM spectra and targeted HCD FT MS/MS using LipidXplorer software (Herzog et al., 2011) PC, PE, SM, PS were quantified by FT MS; free cholesterol, DAG and PI[4]P by HCD FT MS/MS.

Preparation of Giant Unilamellar Vesicles (GUVs). GUVs were generated from liposomes by the electro-swelling method (Bacia et al., 2004). 10–20 µl of liposomes were dried onto two Indium tin oxide-slides (Präzisions Glas & Optik, Germany) by 20 min desiccation under vacuum. Separated by a rubber ring spacer, the slides were assembled together, and 600 µl of 330 mM sucrose were added between the slides. GUVs were formed from liposomes by applying an alternating electric field (10 Hz, sinusoidal wave, 1.8 V) for 2 h, using a Voltcraft 8202 1-channel-function generator (Conrad Electronic, Germany). Subsequently, the GUV containing solution was recovered and diluted in 2 volumes of recruitment buffer. GUVs were allowed to settle down for 30 min, and 200 µl GUV suspension were recovered from the bottom of the tube.

GUV recruitment assays. Cytosol (4 mg/ml) from cells expressing the GFP-tagged protein of interest was clarified by centrifugation at 150,000 g for 30 min. ATP-regeneration system or inhibitors were added as indicated, and the mixture was placed into the wells of an 8-well Lab-Tek glass bottom chamber (Nunc, Germany, pre-coated with 10 mg/ml BSA at 37°C for 1 h.) 10 µl GUV suspension was added to 100 µl of cytosol, and mixed by pipetting up and down. After 20 min incubation at 37°C, the GUVs were analyzed by confocal microscopy.

Microscopy: For microscopy of fixed samples, cells were seeded on 12 mm, No 1.5 glass coverslips (Menzel GmbH, Thermo Scientific, Germany). Cells were washed with PBS, fixed with 4% (w/v) paraformaldehyde in PBS (15 min at room temperature), permeabilized with ice cold 0.1% (v/v) Triton X-100 in PBS (5 min) and then blocked with 3% (w/v) BSA in PBS (20-30 min). For labeling with anti-PI[4,5]P2 and anti-PIP5K1A, cells were washed during all steps with TBS, fixed with 4% (w/v) paraformaldehyde in PBS (15 min), permeabilized with 0.5% saponin (Sigma) for 15 min at room temperature, and blocked with 3% (w/v) BSA in PBS. Cells were incubated with the primary antibody (1 hour at room temperature), washed 3 times (5 min) with PBS, and then labeled with secondary antibodies and DAPI (30 min at room temperature). Subsequently cells were mounted on microscopy slides using MOWIOL (Calbiochem/Merck). Cells were imaged using a LSM 700 or a LSM780 microscope equipped with a 63x 1.4 numerical aperture (NA) or a 100x 1.45 NA Plan-Apochromat objective (Carl Zeiss Microimaging, Germany). For quantifying PI[4,5]P2 on GFP-MPR TGN membranes, 3D renditions were obtained from 0.5 μ m Z-sections using the ImageJ 3D Viewer plugin (volume view) (Rasband, W.S., ImageJ, U. S. National Institutes of Health, Bethesda, Maryland, USA, <http://imagej.nih.gov/ij/>, 1997-2016). The GFP-MPR positive area was selected, and the number and area of objects within this area was calculated. GUVs were analyzed with 40x 1.2 NA water-immersion objective (Carl Zeiss Microimaging). For quantifying p34-Arc on GFP-MPR TGN membranes, 3D renditions were obtained from 0.5 μ m Z-sections using the Volocity software (PerkinElmer, MA, USA). The number of objects within the GFP-MPR positive TGN volume was calculated using Image J. The maximum projection of the GFP-MPR in the Z-stack was used to select a region of interest within each image. The number of objects within this region was calculated for the entire Z-stack using the Object Counter 3D plugin (Bolte and Cordelières, 2006). The Golgi region was identified using GM130 staining, and the area covered by GFP-MPR in this region, as well as the total cell area were measured using ImageJ. The ratio between the two areas was calculated.

For live cell imaging, 60,000 – 120,000 cells were plated on 3.5 cm No. 1.5 glass bottom dishes (MaTek Corporation, MA, USA). Before imaging, cells were washed with PBS and DMEM without phenol red was added. High-speed time-lapse microscopy was performed with either an AFLX6000 microscope equipped with an EMCCD detector, with temperature, CO₂ and humidity control, using a 63x 1.4 NA or a 100x 1.4 NA oil-immersion objective (Leica Microsystems, Germany), or with an Axiovert 200 M with temperature, CO₂ and humidity control and a 63x 1.4 NA Plan-Apochromat objective (Carl Zeiss Microimaging). Movies S3 and 4 were acquired using spinning disk microscopy (PICT-IBiSA Imaging Facility, Paris, France). We used a fast scanning confocal with a spinning disk system mounted on the Ti Eclipse Nikon microscope equipped with perfect focus system and a CCD Coolsnap HQ2 camera and a 100X, 1.45 NA objective (Nikon, Japan).

RAC1 activation assay. GFP-MPR expressing cells were treated with the indicated siRNAs (20 nM) and Interferin. After 3 days, cells were detached and transferred on 10 cm plates coated (30 min, 37°C) with 5 μ g/ml fibronectin (Applichem, Germany). After 3.5 -4h, cells were washed two times with 5 ml ice-cold washing buffer (25 mM Tris pH 7.5, 30 mM MgCl₂, 40 mM NaCl), then cells from each plate were collected in 250 μ l lysis buffer: 50 mM TrisHCl, pH 7.2, 1% (w/v) Triton X-100, 300 mM NaCl, 10 mM MgCl₂, complete protease inhibitors (Roche, Germany), 1 mM PMSF, 8 mM sodium fluoride, 2 mM sodium orthovanadate, 2 mM sodium pyrophosphate (Sigma-Aldrich). Cells were lysed by passing through a 27G needle. Lysates were centrifuged at 14,000 g for 5 min, and the supernatant was collected. 10 μ l PAK-GST beads (1 mg/ml, Cytoskeleton Inc., CO, USA) were added to each tube. Samples were incubated on the rotator (1h, 4°C), beads were collected by centrifugation (8000 g, 1min, 4°C), washed twice with 500 μ l washing buffer with protease and phosphatase inhibitors, re-suspended in 25 μ l 4X Laemmli buffer and analyzed by SDS-PAGE and Western blot.

SUPPLEMENTAL REFERENCES

- BACIA, K., SCHERFELD, D., KAHYA, N. & SCHWILLE, P. 2004. Fluorescence correlation spectroscopy relates rafts in model and native membranes. *Biophys J*, 87, 1034-43.
- BALLA, A., TUYMETOVA, G., TSIOMENKO, A., VARNAL, P. & BALLA, T. 2005. A plasma membrane pool of phosphatidylinositol 4-phosphate is generated by phosphatidylinositol 4-

- kinase type-III alpha: studies with the PH domains of the oxysterol binding protein and FAPP1. *Mol Biol Cell*, 16, 1282-95.
- BOLTE, S. & CORDELIÈRES, F. P. 2006. A guided tour into subcellular colocalization analysis in light microscopy. *J Microsc*, 224, 213-32.
- COX, J. & MANN, M. 2008. MaxQuant enables high peptide identification rates, individualized p.p.b.-range mass accuracies and proteome-wide protein quantification. *Nat Biotechnol*, 26, 1367-72.
- CZUPALLA, C., MANSUKOSKI, H., RIEDL, T., THIEL, D., KRAUSE, E. & HOFLACK, B. 2006. Proteomic analysis of lysosomal acid hydrolases secreted by osteoclasts: implications for lytic enzyme transport and bone metabolism. *Mol Cell Proteomics*, 5, 134-43.
- DAWSON, R. M. & EICHBERG, J. 1965. Diphosphoinositide and triphosphoinositide in animal tissues. Extraction, estimation and changes post mortem. *Biochem J*, 96, 634-43.
- FOLCH, J., LEES, M. & SLOANE STANLEY, G. H. 1957. A simple method for the isolation and purification of total lipides from animal tissues. *J Biol Chem*, 226, 497-509.
- GALLEGOS, L. L., KUNKEL, M. T. & NEWTON, A. C. 2006. Targeting protein kinase C activity reporter to discrete intracellular regions reveals spatiotemporal differences in agonist-dependent signaling. *J Biol Chem*, 281, 30947-56.
- GONZALEZ-SASTRE, F. & FOLCH-PI, J. 1968. Thin-layer chromatography of the phosphoinositides. *J Lipid Res*, 9, 532-3.
- HERZOG, R., SCHWUDKE, D., SCHUHMANN, K., SAMPAIO, J. L., BORNSTEIN, S. R., SCHROEDER, M. & SHEVCHENKO, A. 2011. A novel informatics concept for high-throughput shotgun lipidomics based on the molecular fragmentation query language. *Genome Biol*, 12, R8.
- HUBNER, N. C., BIRD, A. W., COX, J., SPLETTSTOESSER, B., BANDILLA, P., POSER, I., HYMAN, A. & MANN, M. 2010. Quantitative proteomics combined with BAC TransgeneOmics reveals in vivo protein interactions. *J Cell Biol*, 189, 739-54.
- KAWANO, M., KUMAGAI, K., NISHIJIMA, M. & HANADA, K. 2006. Efficient trafficking of ceramide from the endoplasmic reticulum to the Golgi apparatus requires a VAMP-associated protein-interacting FFAT motif of CERT. *J Biol Chem*, 281, 30279-88.
- LANGE, S., SYLVESTER, M., SCHUMANN, M., FREUND, C. & KRAUSE, E. 2010. Identification of phosphorylation-dependent interaction partners of the adapter protein ADAP using quantitative mass spectrometry: SILAC vs (18)O-labeling. *J Proteome Res*, 9, 4113-22.
- MACHACEK, M., HODGSON, L., WELCH, C., ELLIOTT, H., PERTZ, O., NALBANT, P., ABELL, A., JOHNSON, G. L., HAHN, K. M. & DANUSER, G. 2009. Coordination of Rho GTPase activities during cell protrusion. *Nature*, 461, 99-103.
- MATYASH, V., LIEBISCH, G., KURZCHALIA, T. V., SHEVCHENKO, A. & SCHWUDKE, D. 2008. Lipid extraction by methyl-tert-butyl ether for high-throughput lipidomics. *J Lipid Res*, 49, 1137-46.
- MOOTHA, V. K., LINDGREN, C. M., ERIKSSON, K. F., SUBRAMANIAN, A., SIHAG, S., LEHAR, J., PUIGSERVER, P., CARLSSON, E., RIDDERSTRALE, M., LAURILA, E., HOUSTIS, N., DALY, M. J., PATTERSON, N., MESIROV, J. P., GOLUB, T. R., TAMAYO, P., SPIEGELMAN, B., LANDER, E. S., HIRSCHHORN, J. N., ALTSHULER, D. & GROOP, L. C. 2003. PGC-1alpha-responsive genes involved in oxidative phosphorylation are coordinately downregulated in human diabetes. *Nat Genet*, 34, 267-73.
- NIEHAGE, C., STANGE, C., ANITEI, M. & HOFLACK, B. 2014. Liposome-based assays to study membrane-associated protein networks. *Methods Enzymol*, 534, 223-43.
- ROUSER, G., SIAKOTOS, A. N. & FLEISCHER, S. 1966. Quantitative analysis of phospholipids by thin-layer chromatography and phosphorus analysis of spots. *Lipids*, 1, 85-6.
- ROZELLE, A. L., MACHESKY, L. M., YAMAMOTO, M., DRIESSENS, M. H., INSALL, R. H., ROTH, M. G., LUBY-PHELPS, K., MARRIOTT, G., HALL, A. & YIN, H. L. 2000. Phosphatidylinositol 4,5-bisphosphate induces actin-based movement of raft-enriched vesicles through WASP-Arp2/3. *Curr Biol*, 10, 311-20.
- STAUFFER, T. P., AHN, S. & MEYER, T. 1998. Receptor-induced transient reduction in plasma membrane PtdIns(4,5)P2 concentration monitored in living cells. *Curr Biol*, 8, 343-6.
- SUBRAMANIAN, A., TAMAYO, P., MOOTHA, V. K., MUKHERJEE, S., EBERT, B. L., GILLETTE, M. A., PAULOVICH, A., POMEROY, S. L., GOLUB, T. R., LANDER, E. S. & MESIROV, J. P. 2005. Gene set enrichment analysis: a knowledge-based approach for interpreting genome-wide expression profiles. *Proc Natl Acad Sci U S A*, 102, 15545-50.
- SZENTPETERY, Z., VARNAI, P. & BALLA, T. 2010. Acute manipulation of Golgi phosphoinositides to assess their importance in cellular trafficking and signaling. *Proc Natl Acad Sci U S A*, 107, 8225-30.

- WAGURI, S., DEWITTE, F., LE BORGNE, R., ROUILLE, Y., UCHIYAMA, Y., DUBREMETZ, J. F. & HOFLACK, B. 2003. Visualization of TGN to endosome trafficking through fluorescently labeled MPR and AP-1 in living cells. *Mol Biol Cell*, 14, 142-55.
- WHITE, T., BURSTEN, S., FEDERIGHI, D., LEWIS, R. A. & NUDELMAN, E. 1998. High-resolution separation and quantification of neutral lipid and phospholipid species in mammalian cells and sera by multi-one-dimensional thin-layer chromatography. *Anal Biochem*, 258, 109-17.

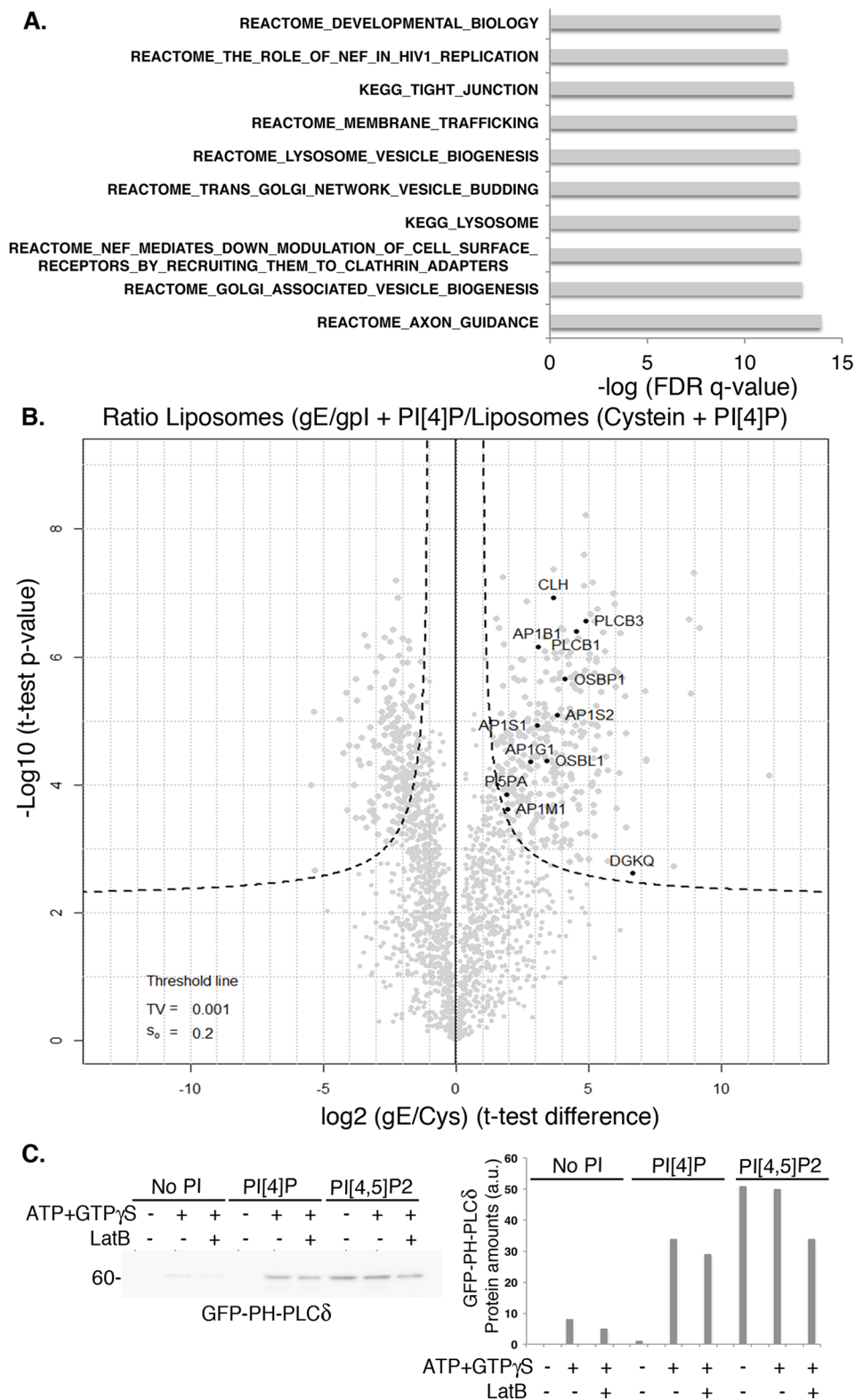


Fig. S1. Protein recruitment on clathrin/AP-1 coated membranes. Related to Figure 1, Table S1 Table S2, and Figure 4. (A) Pathway enrichment of the proteins enriched on flat membranes (-ATP) was calculated using GSEA (see also Fig. 1D, Table S1). The False Discovery Rate (FDR) q-value was calculated for each set. (B) Volcano plot of proteins enriched on liposomes containing AP-1 selective gE/gPI cd peptide compared to control liposomes (Table S2). PI[4]P and PC containing liposomes modified with either gE/gPI cd peptide or cysteine as control, were incubated with mouse brain cytosol in presence of GTPγS and then purified by floatation. Label free quantification of bound proteins was performed (Niehage et al., 2014). Logarithmic (log₂) ratios of protein intensities in the (gE/gPI)/Cys are shown on the X-axis, and the negative logarithmic (log₁₀) p-values of the *t*-test from triplicates on the Y-axis; TV, s₀, represent threshold values (Hubner et al., 2010). Proteins significantly enriched gE/gPI cd peptide liposomes appear above the threshold line on the upper right. (C) Liposomes containing the gE/gPI cd peptide, SM, and no PI, PI[4]P or PI[4,5]P2 were incubated with cytosol of HEK cells expressing GFP-PLCδ-PH for 15 min, in the indicated conditions. Lipid-binding probe recruitment on liposomes was analyzed by Western blot using anti-GFP antibodies (see Fig. 4A, B). Band intensities were measured using ImageJ and the mean intensities were plotted.

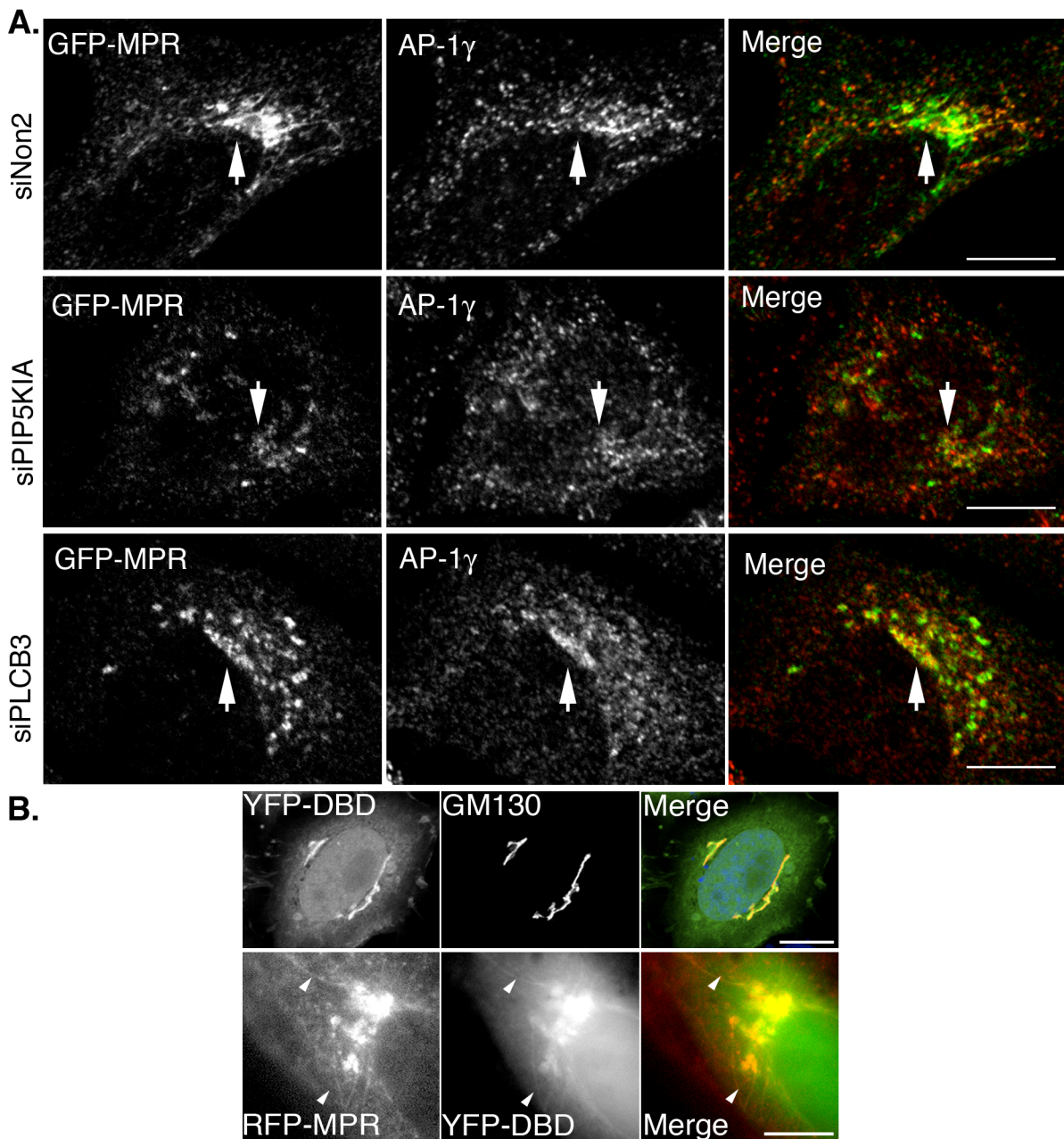


Fig. S2. Knockdowns of PIP5K1A and PLCB3 affect the morphology of the AP-1 coated compartment. Related to Figure 2 and Figure 3. (A) HeLa cells stably expressing GFP-MPR were treated with indicated siRNAs for 72 h, fixed and co-labeled with anti-AP-1 γ (red). Arrows indicate AP-1 γ coated GFP-MPR structures. (B) HeLa cells were transfected with YFP-DBD for 24 h, fixed and co-labeled with anti-GM130 (red, upper panel), or co-transfected with YFP-DBD and RFP-CIMPR (lower panel). Arrowheads indicate TGN-derived MPR positive tubules with bound YFP-DBD (lower panel). Scale bars, 10 μ m.

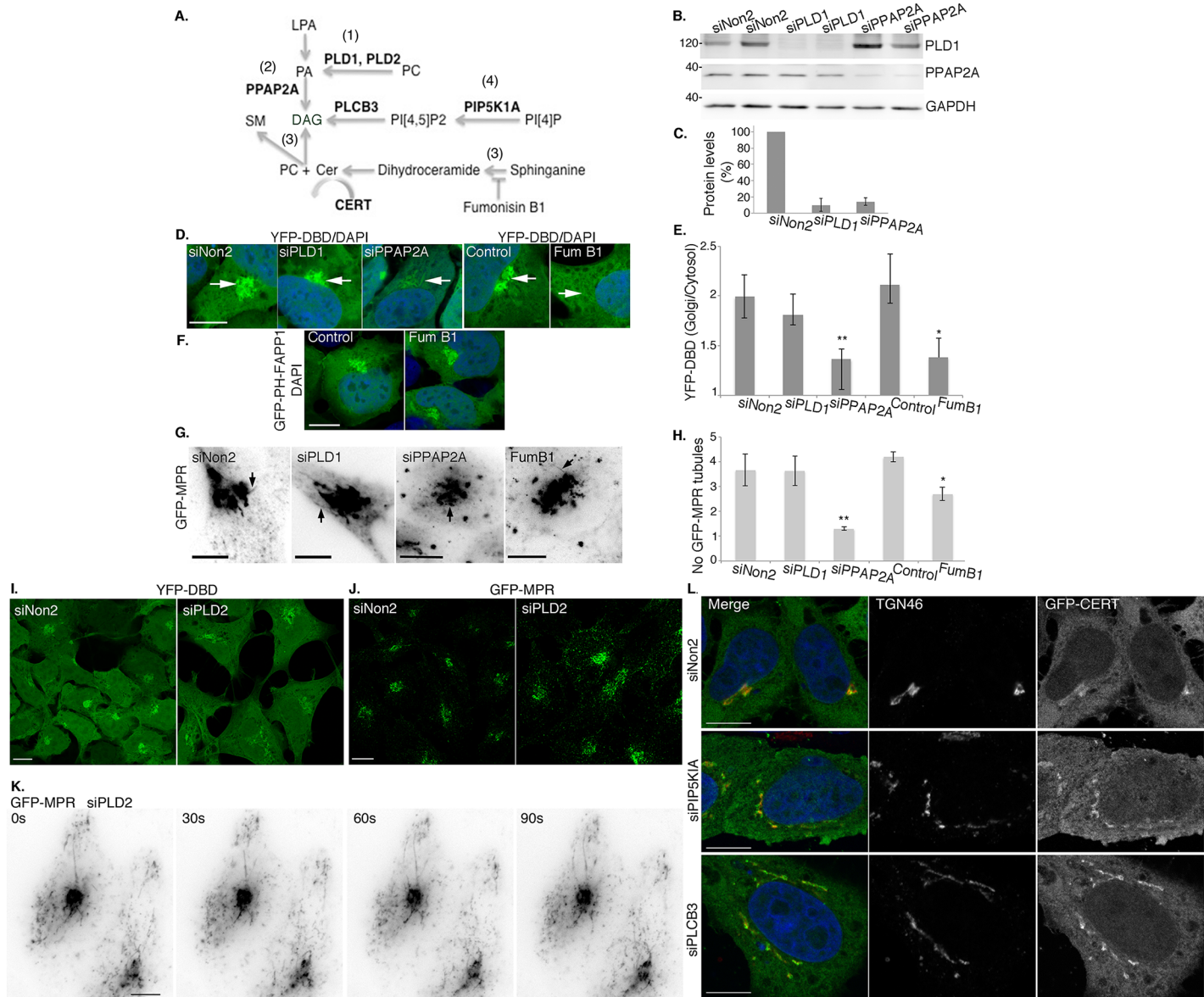


Fig. S3. DAG production on Golgi membranes. Related to Figure 3. (A) Metabolic pathways controlling DAG production on Golgi membranes. (1) PLD1 hydrolyzes PC to PA, which is (2) transformed by phosphatases (i.e. PPAP2A) into DAG. (3) DAG and SM are synthesized from PC and ceramide, a reaction blocked by fumonisins B1. (4) PIP5K1A synthesizes, from PI[4]P, PI[4,5]P2 that is hydrolyzed by PLCB3 to form DAG and IP3. (B) GFP-MPR-expressing cells were treated with the indicated siRNAs for 72 h. Knockdown efficiencies were analyzed by Western blot with anti-PLD1, anti-PPAP2A and anti-GAPDH antibodies. (C) Protein levels were quantified using Image J and are shown relative to control siNon2 ($n = 3$ independent experiments). (D) HEK cells stably expressing YFP-DBD were treated with the indicated siRNAs for 72 h, or with 25 $\mu\text{g/ml}$ of fumonisins B1 for 24 h, then fixed and analyzed using confocal fluorescence microscopy. (E) Fluorescence intensities of YFP-DBD were measured in the Golgi area and in the cytosol using ImageJ. The Golgi/cytosol ratios are shown ($n \geq 3$; ** p -value < 0.001 ; * p -value < 0.05 , ≥ 50 cells/condition). (F) HEK cells stably expressing the GFP-tagged PH domain of FAPP1 were treated with 25 $\mu\text{g/ml}$ fumonisins B1 for 24 h. Cells were fixed and analyzed using confocal fluorescence microscopy. $N = 3$. (G) GFP-MPR-expressing cells were incubated with the indicated siRNAs for 72 h, or with 25 $\mu\text{g/ml}$ fumonisins B1 for 24 h and monitored using live cell imaging (2 min, 0.5 s per frame; Movie S2). (H) The number of TGN-derived tubules formed during 2 min per cell was quantified ($n = 3$; ** p -value < 0.001 ; * p -value < 0.01 , > 50 cells/condition). Data are shown as mean \pm SD. (I, J) HEK cells expressing YFP-DBD (I) and GFP-MPR expressing HeLa cells (J) were incubated with control siNon2 or siPLD2 for 72 h, fixed and analyzed by confocal microscopy. (K) GFP-MPR (black) expressing cells incubated with control siNon2 or siPLD2 for 72 h were analyzed by time-lapse microscopy (2 min, 0.5 s per frame). Images were inverted; $n = 2$ independent experiments in duplicate, > 64 cells/condition. (L) HeLa cells were treated with the indicated siRNAs for 48 h, then transfected with GFP-CERT. After 24 h, cells were fixed and co-labeled with anti-TGN46 (red). Scale bars, 10 μm .

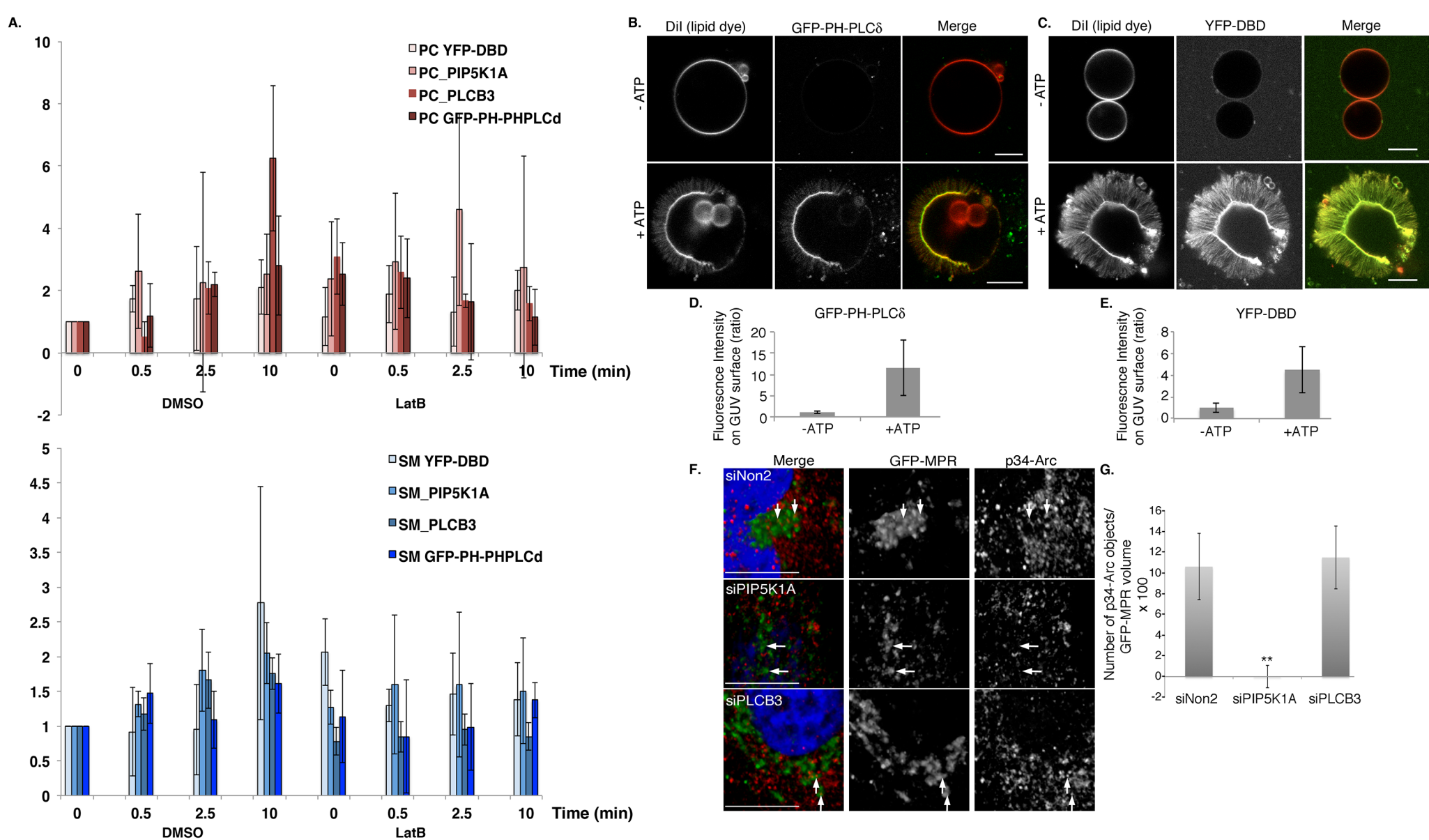


Fig. S4. Analysis of lipid modifications on artificial membranes, and of ARP2/3-dependent actin polymerization in cells. Related to Figure 4 and Figure 5. (A) Quantification of data in Fig. 4A-B. Proteins recruited on liposomes containing PC (upper panel) or SM (lower panel) were analyzed by Western blotting, and protein amounts were quantified using ImageJ ($n = 3-4$ independent experiments). (B-E) GUVs containing PC, the gE/gpI cd peptide and PI[4]P were incubated for 20 min with cytosol from HEK cells stably expressing (B, D) GFP-PLC δ -PH or (C, E) YFP-DBD, GTP γ S and with or without ATP. (D, E) Fluorescence intensities on the GUV surface (25 GUVs per condition) were quantified and are shown as ratios relative to control (-ATP) values (mean \pm SD). (F, G) GFP-MPR expressing HeLa cells treated with the indicated siRNAs were co-labeled with anti-p34-Arc (red). Z-series of 0.5 μ m optical sections were acquired. Images represent a 3D rendition of Z-stacks. (G) The number of p34-Arc-positive objects localized in the GFP-MPR region was calculated in the entire stack and shown as (Number of p34-Arc objects/GFP-MPR volume)*100, median \pm SD ($n = 4$ independent experiments, **p-value = 0.002, > 64 cells/condition). GUVs and cells were analyzed by confocal microscopy. Scale bars, 10 μ m.

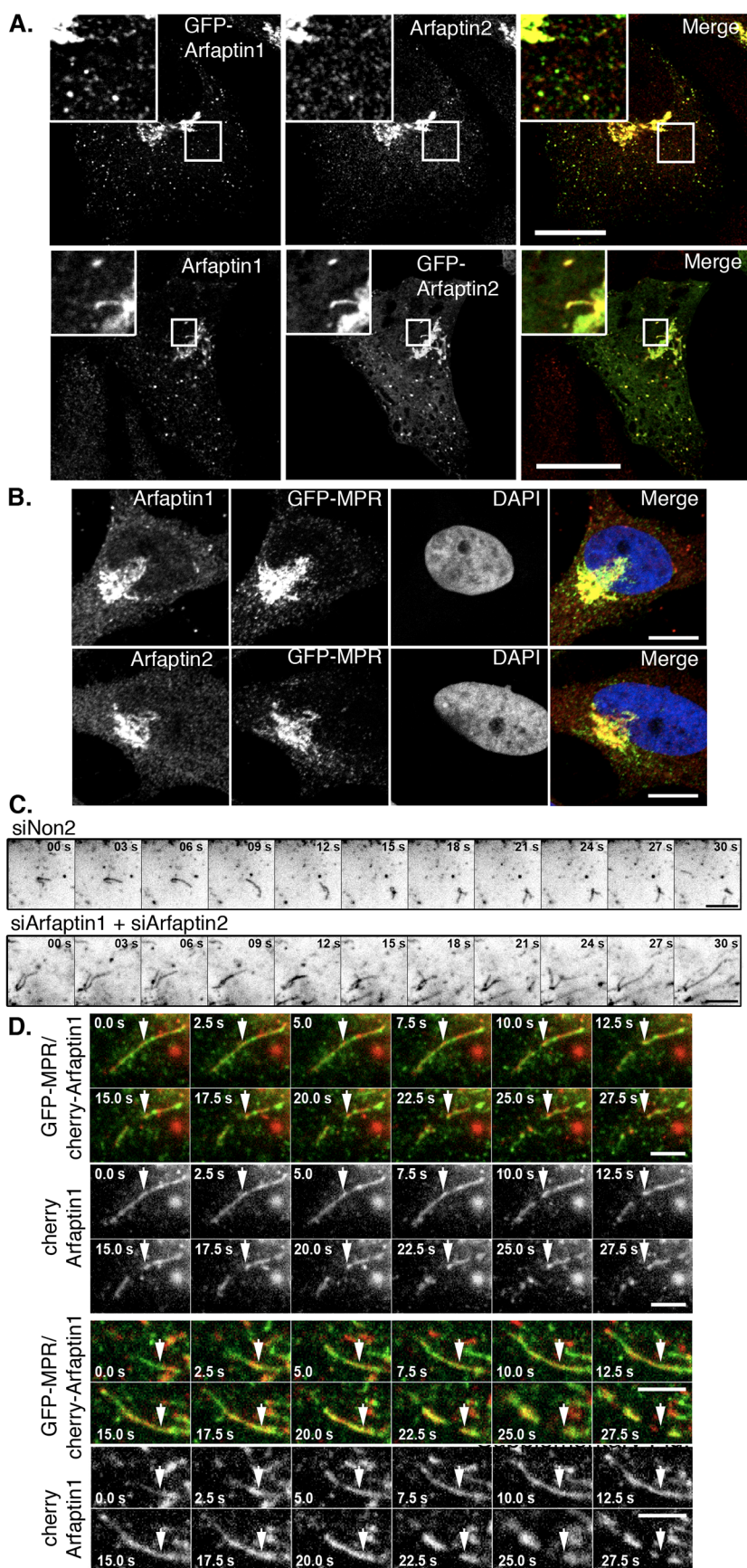


Fig. S5. Localization and dynamics of arfaptin 1/2. Related to Figure 6. (A) HeLa cells were transfected with GFP-arfaptin-1 and labeled with anti-arfaptin-2 antibodies (red), or were transfected GFP-arfaptin-2 and labeled with anti-arfaptin-1 antibodies (red). (B) GFP-MPR cells were labeled with anti-arfaptin-1 or anti-arfaptin-2 antibodies (red). (C) GFP-MPR cells were treated with siRNAs targeting both arfaptin-1 and 2. Representative montages (30 s; 3 s interval) show the dynamics of peripheral tubular carriers. (D) Dynamics of peripheral tubular carriers was studied by time-lapse microscopy in HeLa cells co-transfected with GFP-MPR and mCherry-arfaptin-1. Representative montages (30 s, 2.5 s interval) show carrier fragmentation coinciding with arfaptin-1 subdomain segregation. Arrows indicate arfaptin 1 accumulation along the tubes at sites of membrane scission. Scale bars, (A, B) 10 μ m, (C, D) 5 μ m.